SOLUTION AND APPLICATION OF ANISOTROPIC CURVATURE DRIVEN EVOLUTION OF CURVES (AND SURFACES)

KAROL MIKULA

Department of Mathematics, Slovak University of Technology,
Radlinského 11, 813 68 Bratislava, Slovakia
E-mail: mikula@vox.svf.stuba.sk

We discuss methods of numerical solution of geometrical equations $v = \beta(\theta, k)$, where v is normal velocity of evolving plane curve with curvature k, θ is the angle of the tangent to the curve with horizontal axis, and β is a smooth function increasing in k. Equations of this type are used to describe important phenomena in physics, material science, artificial inteligence, robotics and image processing. Anisotropic motion of phase interface in free boundary problems with surface tension as well as image smoothing, recognition, segmentation and shape analysis in computer vision are well-known examples. We present approximation schemes and existence and convergence results for the curve evolution leading to the solution of degenerate parabolic problems of slow and fast diffusion type. Approximation of the problem by means of the so called intrinsic heat equation and its numerical solution are discussed too. We also study methods based on level set and phase-field formulations of mean curvature flow, and present a comparison study with the previously mentioned methods and application to image selective smoothing and phase transition problems.

1 Introduction

The aim of this work is to present methods for solving the curve evolution equation

$$v = \beta(\theta, k), \tag{1}$$

where v is (outer) normal velocity of evolving plane closed curve with curvature k (which, by the convention introduced by Angenent and Gurtin [9], has negative sign for convex curves), θ is the angle of the tangent to the curve with horizontal axis and β is a smooth function increasing in k. The study of such curve motion (as well as its 3D generalization to surface evolution depending on mean curvature) is motivated by many applications in which Eq. (1) arises and also by its relation to the minimal surface problem. Examples of applications include the following:

- In the material science dealing with *motion of interface (free boundary)* between solid and liquid phases Eq. (1) corresponds to the so called Gibbs-Thomson law governing crystal growth in undercooling liquid [30,67,14].

Angenent and Gurtin theory of interface motion in thermal superconductivity also uses (1) as a natural tool for describing the evolution of phase boundaries [9]. The dependence of the flow on the curvature k is related to surface tension effects on the interface and the dependence on θ (orientation of interface) introduces anisotropy into the model. The nonlinearity given by the function β expresses e.g a dependence of the kinetic coefficient on the normal velocity. Assuming slow interface velocities, this dependence is linear [9] and Eq. (1) corresponds to classical anisotropic curve evolution governed by

$$\alpha_1(\theta)v = \alpha_2(\theta)k - F, \tag{2}$$

where α_1, α_2, F represent physical quantities comming from constitutive description of interface. In the isotropic case we end up with the classical (i.e linear $v = k$) curve shortening flow [27,1,6,29].

- In the context of image processing, the so-called *morphological image and shape multiscale analysis* is used due to its contrast invariance properties. It has been introduced by Sapiro and Tannenbaum [62] and Alvarez, Guichard, Lions and Morel [2,3,34] as a natural result of axiomatization of computer vision theories. In general, an image silhouette (boundary of distinguished shape) corresponds to a level line of image intensity function. The *morphological scaling* (shape analysis) of the silhouette leads to the equation of the form (1) without anisotropic part. Namely, *affine invariant scale space* has special conceptual meaning and importance. It is a generalization of the linear curve shortening flow, and is given by Eq. (1) provided $\beta(k) = k^{1/3}$ [2,62,63,64,65,11]. In the problems of image segmentation [40,43] also "anisotropic like" models have been used recently [18].

- Models involving Eq. (1) are used also in other applied sciences, e.g. in modelling of flame front propagation in combustion, computing of first arrival times of seizmic vawes, in computational geometry, robotics, semiconductors industry, etc. (for a comprehensive overview of applications we refer to Sethian's book [70]).

From the computational point of view, two main approaches are used for solving Eq. (1):

1. Direct approach, in which the parameters of evolving curve, namely

- position vector in **intrinsic heat equation** [22,23,24,51,52]

or

- curvature in **porous-medium like equation** [46,45]

are unknowns in related initial boundary value problems. There are also direct methods based on the so-called *crystalline curvature* approximation [28,72], special finite difference schemes [41,42] and a method based on *erosion of*

polygons in affine invariant case [53].
2. Level set approach based on introducing of an auxiliary function $\phi(x,t)$, $\phi : \mathbb{R}^d \times \mathbb{R}_0^+ \to \mathbb{R}$ ($d = 2$ or 3) which is an unknown in the so called

- **level set equation** [57,69,70,71,31]

or in the so called

- **phase-field formulations** of the curve and surface evolution in the form of **reaction–diffusion equations** [15,54,58,25,14].

In the level set approach, the zero level set of the function ϕ (namely, isoline in 2D or isosurface in 3D) corresponds to the evolving curve (surface) for any t. The level set equation is used in sharp interface motion modelling while various phase-field equations are used to describe motion of diffussive interface (then the curve evolution by (1) is given as a limit when thickness of diffusive interface goes to zero).

In the next sections, we discuss the concepts and computational methods which can be used for dealing with the main approaches mentioned above.

2 Direct approach using porous-medium like equations

In order to model the curve evolution we consider a vector function $x(u,t)$, $x : \mathbb{R} \times [0, T_{max}) \to \mathbb{R}^2$ periodic in the first argument with a period given by the range of curve parametrization u. Then, $x(u,t)$ corresponds to position vector of the evolving curve $\Gamma = Image(x)$ in time t. Of course, the evolving curve admits various parametrizations. First, let us consider closed and strictly convex initial curve $x(.,0)$. Then, θ - the angle of the tangent to the curve with the horizontal axes - is a convenient parametrization varying in fixed interval $[0, 2\pi\nu]$, where $\nu \in \mathbb{N}$ corresponds to the index of the curve. Let the initial closed strictly convex curve $x^0 = x(\theta, 0)$ be parametrized by θ and let $k_0(\theta)$ be its curvature. Then, using [27,9], we have that the flow $x(\theta,t)$ of the curves, starting from x_0, which solves the problem (1) and remains strictly convex is given uniquely up to a translation by the formula

$$x(\theta_0, t) = x(0,t) - \int_0^{\theta_0} \frac{e^{i\theta}}{k(\theta,t)} d\theta, \tag{3}$$

in which the curvature $k(\theta,t)$ is the solution of the following doubly-nonlinear porous medium type initial boundary value problem:

$$\begin{aligned} \partial_t b(k) &= \partial_{\theta\theta}\beta(\theta,k) + \beta(\theta,k), \\ k(\theta,t) &= k(\theta + 2\pi\nu, t), \\ k(\theta,0) &= k_0(\theta), \end{aligned} \tag{4}$$

with $b(k) = -1/k$. For many so far studied curve evolutions, namely classical linear curve shortening [27], affine invariant scale space [62,11], anisotropic curve shortening [9,10], power like nonlinear curve evolution with positive anisotropy [5,52], the conservation of strict convexity has been proved in mentioned references. The proofs are basically based on application of maximum principle to equations of type (4) or Matano's result [44] which leads to the statement that curvature of evolving curves cannot change sign during the evolution. The nonlinear problem (4) with periodic boundary conditions can be solved numerically by a kind of Jäger-Kačur algorithm [32,36,33,35]. Such approach for solving the curve evolution problem was developed in [46,45] and has been applied to anisotropic as well as nonlinear curve shortening. The discrete curvature function is computed in each discrete time step of the numerical scheme designed to solve Eq. (4) and the curve flow is reconstructed by the formula (3).

Let us briefly recall the main ideas of approximation of Eq. (4). We consider case of separated anisotropy and nonlinearity in the form

$$\beta(\theta, k) = S_1(\theta)\gamma(k) + S_2(\theta),$$

where $S_1 \geq q > 0, S_1', S_1'', S_2$ are bounded measurable functions, periodic in interval $[0, 2\pi\nu]$ and γ is C^2-function in $\mathbb{R} - \{a\}$ with $\gamma'(z) > 0, z \neq a$, $\gamma'(a) \geq 0$, $\gamma(a) = a$.

The mathematical and numerical difficulties are caused by degeneracies in Eq. (4). Namely, asymptotical degeneracy of *slow diffusion type* ($b' = \infty$, $\gamma' = 0$) is related to the parts of the curve, where curvature is close to 0 and plays the role in the presence of anisotropy and porous medium like nonlinearity (e.g. $\gamma(z) = z^m, m > 1$). Asymptotical degeneracy of *fast diffusion type* ($b' = 0$, $\gamma' = \infty$) is related to both, large and small curvatures, and plays the role near the shrinking, singularities formation and influences a more shape preserving (e.g. affine invariant, $\beta(k) = k^{1/3}$) evolution. The special form of the problem causes a blow up of the curvature in a finite time which corresponds to the shrinking of the curve to a point or to other singular behaviour.

If we denote $I = [0, T_{max}]$, $J = [0, 2\pi\nu]$, $Q_T = I \times J$, $V = \{w \in W_2^1(0, 2\pi\nu) : w(0) = w(2\pi\nu)\}$, V^* its dual space, and assuming that $\gamma(k_0) \in V$, we can define weak solution of (4) as a function $k \in L_2(Q_T)$ with $\partial_t b(k) \in L_2(I, V^*)$ for which $\beta(\theta, k) \in L_2(I, V)$, $k(\theta, 0) = k_0(\theta)$ and

$$\int_I \int_J \partial_t b(k)\varphi d\theta dt + \int_I \int_J \partial_\theta \beta(\theta, k)\varphi_\theta d\theta dt = \int_I \int_J \beta(\theta, k)\varphi d\theta dt, \ \forall \varphi \in L_2(I, V).$$

In order to find the weak solution we use the following **approximation**

scheme for the porous medium like curve evolution equation (4): Let $n \in \mathbb{N}, \tau = \frac{T_{max}}{n}, t_i = i\tau$ for $i = 0, \ldots, n$, $k_0 = k_0(\theta), K_0 = \gamma(k_0)$. For $i = 1, \ldots, n$ we look for the functions $K_i \in V$ $(K_i \approx \gamma(k_i))$, $\mu_i \in L_\infty(\Omega)$ such that

$$\int_J \mu_i(K_i - \gamma(k_{i-1}))\varphi d\theta + \tau \int_J \partial_\theta \tilde{\beta}(\theta, K_i)\varphi_\theta d\theta = \tau \int_J \tilde{\beta}(\theta, K_i)\varphi d\theta, \ \forall \varphi \in V \tag{5}$$

where $\tilde{\beta}(\theta, z) = \beta(\theta, \gamma^{-1}(z)) = S_1(\theta)z + S_2(\theta)$, provided the *convergence condition*

$$\alpha\frac{\lambda}{2} \leq \mu_i \leq \frac{b(\gamma^{-1}(\alpha K_i + (1-\alpha)\gamma(k_{i-1}))) - b(k_{i-1})}{K_i - \gamma(k_{i-1})}, \tag{6}$$

holds with $0 < \alpha < 1$ (α close to 1) and λ is a lower bound of derivative of a regularized $b \circ \gamma^{-1}$ function [46,45]. The curvature function k_i is obtained by the *algebraic correction*

$$b(k_i) := b(k_{i-1}) + \mu_i(K_i - \gamma(k_{i-1})). \tag{7}$$

In this scheme, the nonlinearity of equation is treated by the optimal choice of relaxation function μ_i corresponding to $\partial_z(b \circ \gamma^{-1})$ constructed in an iterative way [45,46]. Using k_i, K_i obtained in each time step of (5)-(7), the Rothe functions

$$\overline{k}^{(n)}(t) = k_i, \text{for } t_{i-1} < t \leq t_i, i = 1, \ldots, n, \ \ \overline{k}^{(n)}(0) = k_0, \tag{8}$$

$$\overline{K}^{n}(t) = K_i, \text{for } t_{i-1} < t \leq t_i, i = 1, \ldots, n, \ \ \overline{K}^{n}(0) = K_0 \tag{9}$$

are constructed. Then due to [46,45] we have

$$\overline{k}^{(n)} \to k \ \text{ in } L_2(Q_T), \quad \overline{K}^{n} \to \gamma(k) \ \text{ in } L_2(I, V),$$

where k is unique bounded weak solution of the initial-boundary value problem (4). The linear elliptic convection-diffusion equation (5) can be solved by finite element discretization or by finite volume method including the so-called upwind principle.

3 Direct approach by intrinsic heat equations

In the concept presented above, the existence and uniqueness of the solution as well as convergence and error estimates of approximations are proved [46,45]. However, such approach holds only for convex curve motions and, from practical point of view, we would like to handle general nonconvex curve evolution governed by Eq. (1). In the nonconvex case, θ–parametrization seems to be not convenient due to a changing of its range during the evolution for each convex/concave piece of a curve. Another idea, originating in Dziuk's algorithm for evolutionary surfaces can be used. Provided $\beta = \beta(k)$, we use the representation of Eq. (1) by the so called *intrinsic heat equation* [51]

$$\frac{\partial x}{\partial t} = \frac{\partial^2 x}{\partial s_*^2} \tag{10}$$

where s_* is a special curve parametrization related to standard arc-length parametrization by

$$ds_* = \vartheta(s)ds, \vartheta = k^{1/2}\beta(k)^{-1/2}.$$

Then clearly

$$\frac{\partial x}{\partial t} = \frac{1}{\vartheta(s)}\frac{\partial}{\partial s}\left(\frac{1}{\vartheta(s)}\frac{\partial x}{\partial s}\right) = \beta(k)N - \frac{\vartheta'(s)}{\vartheta^3(s)}T$$

where T is the unit tangent vector, $T = x_s$ and N is the unit normal vector satisfying Frenet's formula $T_s = kN$. Hence the normal velocity $v = (\frac{\partial x}{\partial t}, N)$ fulfills (1).

Let $u \in [0,1]$ be a time independent parametrization of a curve Γ. Then the arc-length parametrization s of Γ is related to u by $ds = |x_u|du$. Let us define scalar valued function $G : \mathbb{R}^2 \times \mathbb{R}^2 \to \mathbb{R}_0^+$,

$$G(p,q) = |p|k(p,q)^{1/2}\beta(k(p,q))^{-1/2}$$

where

$$k(p,q) = |p|^{-3}\left(|p|^2|q|^2 - (p,q)^2\right)^{1/2} \quad p,q \in \mathbb{R}^2$$

and $(.,.)$ denotes the Euclidean scalar product in $\mathbb{R}^2$ and the corresponding norm is denoted by $|.|$. With this notation, (10) can be rewritten as follows

$$\frac{\partial x}{\partial t} = \frac{1}{G(x_u,x_{uu})}\frac{\partial}{\partial u}\left(\frac{1}{G(x_u,x_{uu})}\frac{\partial x}{\partial u}\right), \quad (u,t) \in [0,1] \times [0,T_{max}). \tag{11}$$

The fully nonlinear system of PDE's (11) is subject to the initial condition $x(u,0) = x^0(u), u \in [0,1]$ and periodic boundary conditions at $u = 0,1$.

Approximation scheme for the curve evolution based on intrinsic heat equation:

Let $\tau = \frac{T_{max}}{n}, n \in \mathbb{N}$ denote time discretization step. By $x^i, i = 0,1,...,n$, we denote the approximation of a solution of (11) at time $t = i\tau$, i.e. $x^i(.) = x(.,i\tau)$. The idea of the construction of a time discretization scheme is based on approximation of the intrinsic heat equation (10) by the backward Euler method

$$\frac{x^i - x^{i-1}}{\tau} = \frac{\partial^2 x^i}{\partial s_*^2}, \quad i = 1,2,...,n,$$

where the parameterization s_* is computed from the previous time step x^{i-1}. The semidiscrete scheme thus reads as follows

$$x^i - \frac{\tau}{G^{i-1}} \frac{\partial}{\partial u}\left(\frac{1}{G^{i-1}} \frac{\partial x^i}{\partial u}\right) = x^{i-1}, \quad i = 1, 2, ..., n, \tag{12}$$

where $G^{i-1} = G(x_u^{i-1}, x_{uu}^{i-1})$ and x^0 is the initial condition.

One can prove that the length of the curve $\Gamma^i = Image(x^i)$ decreases along the semidiscrete evolution generated by (12) [51]. It represets a kind of stability property for the scheme. To derive the fully discrete analogue of (12) we use the uniform spatial grid $u_j = jh$ $(j = 0, ..., m)$ with $h = 1/m$. The smooth solution x is then approximated by the discrete values x_j^i corresponding to $x(jh, i\tau)$. Using finite difference approximations of spatial differential terms in (12) we end up with the following semi-implicit fully discrete scheme

$$\frac{1}{2}(G_j^{i-1} + G_{j+1}^{i-1}) \frac{x_j^i - x_j^{i-1}}{\tau} = \frac{x_{j+1}^i - x_j^i}{G_{j+1}^{i-1}} - \frac{x_j^i - x_{j-1}^i}{G_j^{i-1}} \tag{13}$$

$i = 1, ..., n, j = 1, ..., m$, where (we slightly regularize G_j^{i-1} in order to avoid zeroes in denominator)

$$G_j^{i-1} = h_j^{i-1} \sqrt{\frac{k_j^{i-1} + \varepsilon}{\beta(k_j^{i-1} + \varepsilon)}}, \quad h_j^{i-1} = |x_j^{i-1} - x_{j-1}^{i-1}|,$$

$$k_j^{i-1} = \frac{\left|\arccos\left((x_{j+1}^{i-1} - x_{j-1}^{i-1}, x_j^{i-1} - x_{j-2}^{i-1})/(|x_{j+1}^{i-1} - x_{j-1}^{i-1}||x_j^{i-1} - x_{j-2}^{i-1}|)\right)\right|}{h_j^{i-1}}.$$

The scheme is subject to the periodic boundary conditions $x_{j+m}^i = x_j^i$ $(j = 0, 1)$. In each discrete computational time step $i\tau$ the scheme (13) leads to solving of two tridiagonal systems for the new curve position, which are computed in a very fast way. Let us mention that (13) does not involve the spatial grid parameter h (i.e. the scheme respects the intrinsic character of the equation) and in the linear case $\beta(k) = k$ it coincides with Dziuk's scheme [23]. Recently, the approach based on intrinsic heat equation has been adopted also to anisotropic motion for general case (1) [52] and to anisotropic case with linear $\gamma(k) = k$ [24].

In the end of this section we present several computational results related to the schemes (5)-(7) and (13). They show good correspondence of both methods in convex case (until formation of singularities) and also successful computation of nonconvex curves evolution.

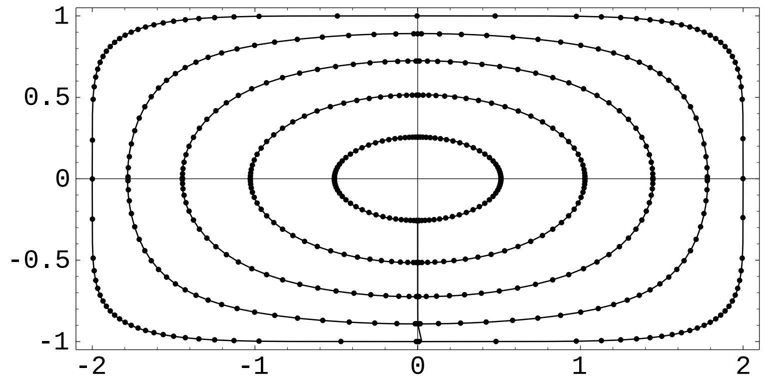

Figure 1. Comparison of two different methods for evolution of convex curve; tick marks - method (13), solid lines - method (5)-(7), affine invariant case $\beta(k) = k^{1/3}$. We also remark proper redistribution of flowing points representing the discrete curve in the method (13) due to the presence of tangential velocity

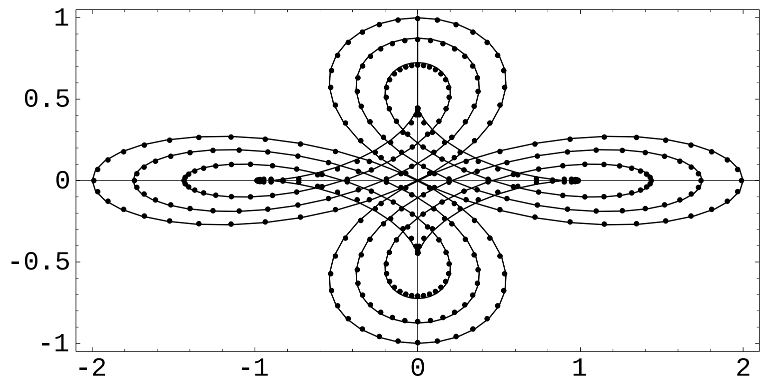

Figure 2. Comparison of two different methods for evolution of selfintersecting "convex" curve, $\beta(k) = k^{1/3}$. Tick marks - method (13), solid lines - method (5)-(7). The evolving curve is plotted at the same discrete time moments until the "hair" singularity is formed. The method (5)-(7) cannot continue beyond singularity.

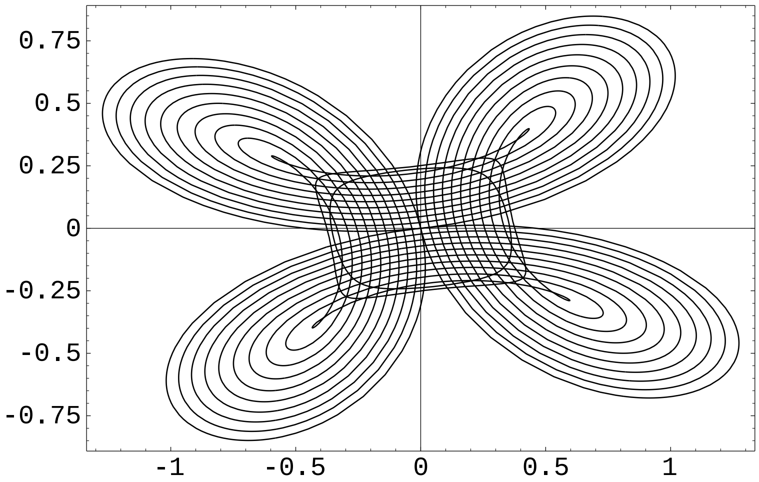

Figure 3. Evolution of the affine transformed 4-petal through singularities computed by the method (13), $\beta(k) = k^{1/3}$.

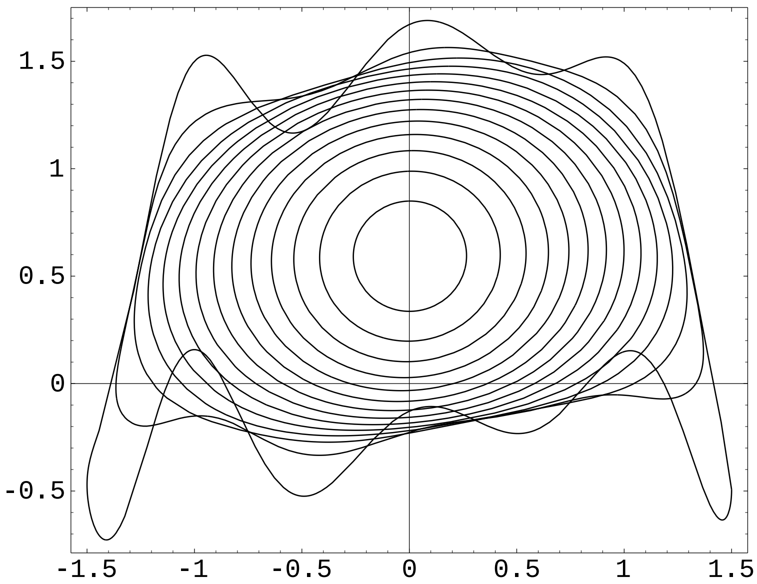

Figure 4. The evolution of initial nonconvex plane curve computed by the method (13), $\beta(k) = k$.

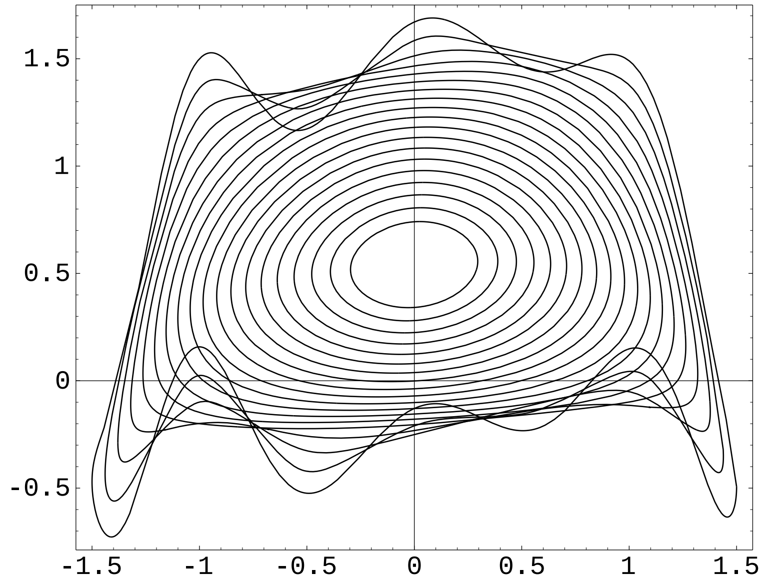

Figure 5. The evolution of initial nonconvex plane curve computed by the method (13) to ellipse rounded point. The affine invariant case $\beta(k) = k^{1/3}$.

4 Solution using level set equation

The direct approach, called also *Lagrangean*, described in previous two sections is very efficient and computationally fast method. However, it can hardly handle splitting and/or merging of curves or surfaces during the evolution (e.g in modeling of phase transition). In spite of this, level set approach, called also *Eulerian*, allows to overcome this difficulty. It handles implicitly the curvature driven motion passing the problem to higher dimensional space. The *level set method* of Osher and Sethian [57,69,70,71] and *phase field models* [15,54,25,14] are approaches of such type.

The main idea of the level set method is to look for the function $\phi : \mathbb{R}^2 \times \mathbb{R}_0^+ \to \mathbb{R}$, for which the moving curve x is the same level line at each time moment t, i.e.

$$\phi(x(t), t) = c \tag{14}$$

for every $t \in I$ and certain $c \in \mathbb{R}$. As initial datum for ϕ we can consider e.g. the so-called signed distance function given by

$$\phi(x,0) = \pm d(x), \tag{15}$$

where $d(x)$ is distance from the point x to the initial curve Γ and the plus (minus) sign is chosen if the point x is outside (inside) the initial curve Γ. Differentiating (14) in time one gets

$$\nabla\phi.\frac{\partial x}{\partial t} + \frac{\partial \phi}{\partial t} = 0. \tag{16}$$

Since only normal component of velocity of flowing curve point influences image of the evolution [65] we can write Eq. (1) in the form

$$\frac{\partial x}{\partial t} = \beta(\theta, k)N. \tag{17}$$

We have also

$$N = \frac{\nabla\phi}{|\nabla\phi|} \tag{18}$$

holding for outer normal vector N to the level set of ϕ. Using (17) and (18) in (16) we obtain the following Hamilton-Jacobi partial differential equation

$$\frac{\partial \phi}{\partial t} + \beta(\theta, k)|\nabla\phi| = 0 \tag{19}$$

for the unknown function ϕ. This equation is a basis for construction of the Osher-Sethian numerical *level set method* [57,69] for solving (1). They used ideas of the so-called up-wind schemes for nonlinear conservation laws to solve (19) numerically. Due to the relation

$$k = -\nabla\left(\frac{\nabla\phi}{|\nabla\phi|}\right)$$

which holds for the curvature k of the level line of ϕ passing through point x, provided $\beta(\theta, k) = k$, we get the well-known *level set equation*

$$\frac{\partial \phi}{\partial t} = |\nabla\phi|\nabla\left(\frac{\nabla\phi}{|\nabla\phi|}\right). \tag{20}$$

This equation moves all level lines of ϕ by the normal velocity proportional to its curvature. Up to a constant and with $\phi : \mathbb{R}^3 \times \mathbb{R}_0^+ \to \mathbb{R}$, this equation holds true also for the iso-surfaces evolving by mean curvature (which is given as a sum of principal curvatures of hypersurface). Previous derivation of (20) has been formal assuming that all terms are well defined and smooth enough. In general situation one has to use theory of the so-called viscosity solutions [19] in order to define in a proper way a solution of the level set equation [26,17].

Let us note that (20) represents a special type of diffusion process. If we fix coordinate system in point $x \in \mathbb{R}^2$ on a level line of ϕ in such a way that ξ, the first coordinate vector is identical with tangent to the level line and the second coordinate vector η corresponds to its normal, then the differential operator $|\nabla\phi|\nabla.\left(\frac{\nabla\phi}{|\nabla\phi|}\right)$ can be rewritten as $\frac{\partial^2\phi}{\partial\xi^2}$. It means that (20) diffuses the solution ϕ in the direction tangential to the level lines and there is no diffusion in the direction orthogonal to them. This idea is used strongly in image selective smoothing, because our auxiliary function ϕ can represent greylevel image intensity function and then level lines of ϕ represent silhouettes of the image [2,4,3,47,31]. Eq. (20) diffuses image along silhouettes without any blurring of them. However silhouettes themselves (as curves or surfaces) are smoothed. We know that (1) is the intrinsic heat equation on curve and thus it represents a kind of *Gaussian smoothing* of the curve itself. We use such ideas to process echo-cardiographic images in 2D and 3D in order to extract smooth shapes of left ventricle of human heart. We solve numerically Evans-Spruck's type regularization of slightly more general equation as (20), namely the problem [31]

$$\frac{1}{\sqrt{\varepsilon + |\nabla\phi|^2}}\phi_t - g(|\nabla\phi|)\nabla.(\frac{\nabla\phi}{\sqrt{\varepsilon + |\nabla\phi|^2}}) = 0 \text{ in } I \times \Omega, \tag{21}$$

where $1 > \varepsilon > 0$ is a (small) real number, $I = [0, T_{max}]$ is the so-called scale interval, $\Omega \subset \mathbb{R}^d$ is an image domain and g is smooth, positive, decreasing function, $g(s) \to 0$ for $s \to \infty$. Eq. (21) is accompanied with homogeneous Neumann boundary conditions and initial condition given by greylevel intensity function of the processed image.

As an example of application, we visualize level surface which represents the boundary of the volume containing blood in one moment of cardiac cycle. On the left side of Figure 6, the unfiltered isosurface is plotted. There are many nonrealistic fingers, incisions and peaks caused by aquisition. We move such surface in the direction of its normal vector field with the velocity proportional to the mean curvature. The motions of convex and concave pieces are opposite due to the curvature sign, and the large fingers shrink faster due to the curvature dependence of flow. Thus, locally in scale, we can obtain reasonable smoothing of the isosurface. The result of such image processing is plotted in the right side of Figure 6.

On the other hand, model (21) can be used successfully for image selective smoothing with conserving of edge positions [59,16,4,37,38,12]. The function $g(s)$ depending on $|\nabla\phi|$ - edge indicator is used to "stop" the motion of silhouette-edge (i.e. the motion of level line on which the image intensity gradient is large). The regions between edges are smoothed due to the diffusion process.

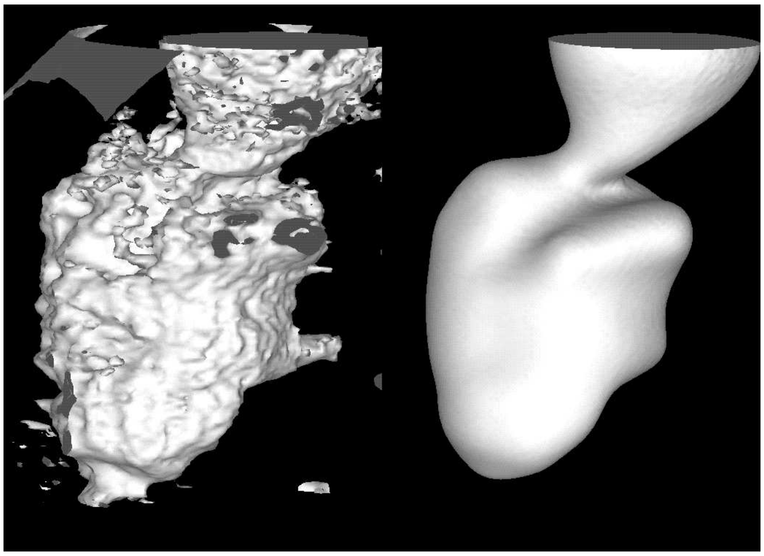

Figure 6. The heart ventricle in open phase - visualized from the result of aquizition (left) and after 3D image processing by mean curvature flow (right).

Here, we present Figure 7 where two chromozomes are extracted from an initial noisy 3D-image by selective smoothing (21) with $g(s) = 1/(1+s^2)$.

The models like (21) are strongly inspired by the original work of Perona and Malik [59] where first nonlinear partial differential equation has been suggested for image selective smoothing and edge detection. Perona and Malik have considered equation of the form

$$\phi_t = \nabla(g(|\nabla\phi|)\nabla\phi) \tag{22}$$

which is called usually *anisotropic diffusion* in computer vision community.

The nonlinear diffusion term in (22)can be rewritten as [2]

$$\nabla(g(|\nabla\phi|)\nabla\phi) = g(|\nabla\phi|)\phi_{\xi\xi} + G'(|\nabla\phi|)\phi_{\eta\eta} \tag{23}$$

where $G(s) = sg(s)$ and ξ, η are tangential and orthogonal vectors to the level line, respectively. From this form one can simply see how diffusion behaves along and across image silhouettes with different choices of g. There is always positive but possibly strongly slowed-down diffusion *along* level lines representing silhouette-edges. *Across* such silhouettes, there can be either forward diffusion (not too interesting from the point of image enhancement), zero diffu-

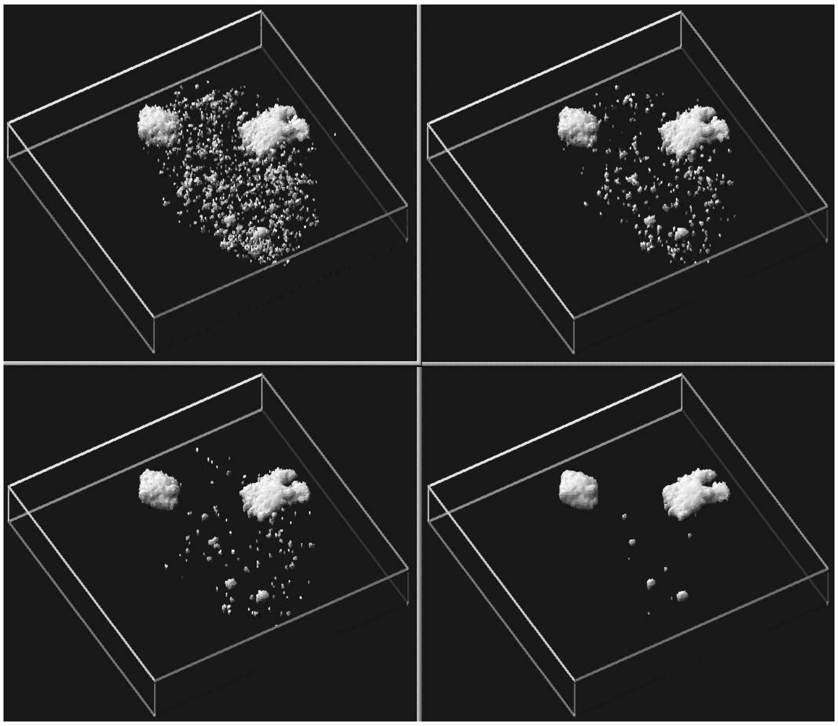

Figure 7. Extraction of the chromozomes from 3D image by mean curvature flow with velocity depending on the gradient of solution.

sion (in Rudin-Osher-Fatemi model [61,56], where $g(s) = 1/s$) or backward diffusion (in the original Perona–Malik choice, where $g(s) = 1/(1+s^2), g(s) = e^{-s}$). The character of diffusion depends on monotonicity of $G(s)$. If the product $g(s)s$ is a decreasing function then Perona-Malik equation can behave locally like backward heat equation, which is an ill–posed problem. Thus, for g's used in practice ($g(s) = 1/(1 + s^2), g(s) = e^{-s}$) both existence and uniqueness of a solution can not be obtained. However, the model has been used in various numerical implementations in wide range of application especially in medical image processing. One way how to prevent this paradox and mathematical disadvantage was proposed by Catté, Lions, Morel and Coll in [16]. They introduced convolution with *Gaussian kernel* G_σ into the decision process for the value of diffusion coefficient, namely, they suggested the following equation

$$\phi_t - \nabla(g(|\nabla G_\sigma * \phi|)\nabla\phi) = f(\phi^0 - \phi), \tag{24}$$

where $G_\sigma \in C^\infty(\mathbb{R}^d)$ is a smoothing kernel, e.g *Gaussian function*, and by means of f on the right–hand side of (24), the solution ϕ is forced to be close to ϕ^0 [55]. This slight modification allowed them to prove existence and uniqueness of the weak solution for the modified equation (24) and keep all practical advantages of original formulation. Moreover, the usage of the *Gaussian gradient* $\nabla G_\sigma * \phi$ instead of $\nabla\phi$ makes the process more stable in the presence of noise. It has made explicit a *presmoothing* included implicitly in numerical realizations of Perona–Malik equation, too. In [37,12,38,39,49,66,50] we are dealing with numerical solution of (24) and its generalizations together with application to image processing. We have suggested semi-implicit finite element and finite volume schemes using also adaptivity on unstructured grids corresponding to image coarsening strategy. We can prove also convergence of such schemes to a weak solution of (24).

The similar idea for numerical solution has been used also in case of Evans-Spruck regularization of level-set-like equation (21). We solve (21) by a kind of semi-implicit method treating all nonlinearities from the previous scale step [31]. 3D experiments presented in Figures 6 and 7 has been computed by such approximation. We choose discrete scale step τ and in each discrete scale moment $t_i = i\tau$ we solve variational identity

$$\int_\Omega \frac{(\phi_h^i - \phi_h^{i-1})\varphi_h}{g(|\nabla\phi_h^{i-1}|)\sqrt{\varepsilon + |\nabla\phi_h^{i-1}|^2}} + \tau\int_\Omega \frac{\nabla\phi_h^i.\nabla\varphi_h}{\sqrt{\varepsilon + |\nabla\phi_h^{i-1}|^2}} = 0,\ \forall\varphi_h \in V_h \tag{25}$$

for the unknown function $\phi_h^i \in V_h$, where V_h is the space of linear finite elements on triangular (tetrahedral) grid corresponding to image pixel/voxel structure and a kind of mass lumping is used in the first term in (25).

The semi-implicit method (25) can be used for computing the curve evolution equation (1). In Figure 8 we present its comparison with direct method (13). We solve numerically evolution of nonconvex curve plotted on the top left part of Figure 8. As initial function $\phi(x, 0)$ we have chosen signed distance function (15). In the next images (to the right and down) we plot numerical solutions until circular shape is reached and the curve is shrinking into a point. By solid lines we plot solution given by method (25), by dashed lines we present solution given by the scheme (13) (the algorithm (13) is also accompanied with uniform redistribution of curve representation points [52]). From the comparison one can see a precise coincidence of two methods during evolution as well as a correspondence of numerical extinction times.

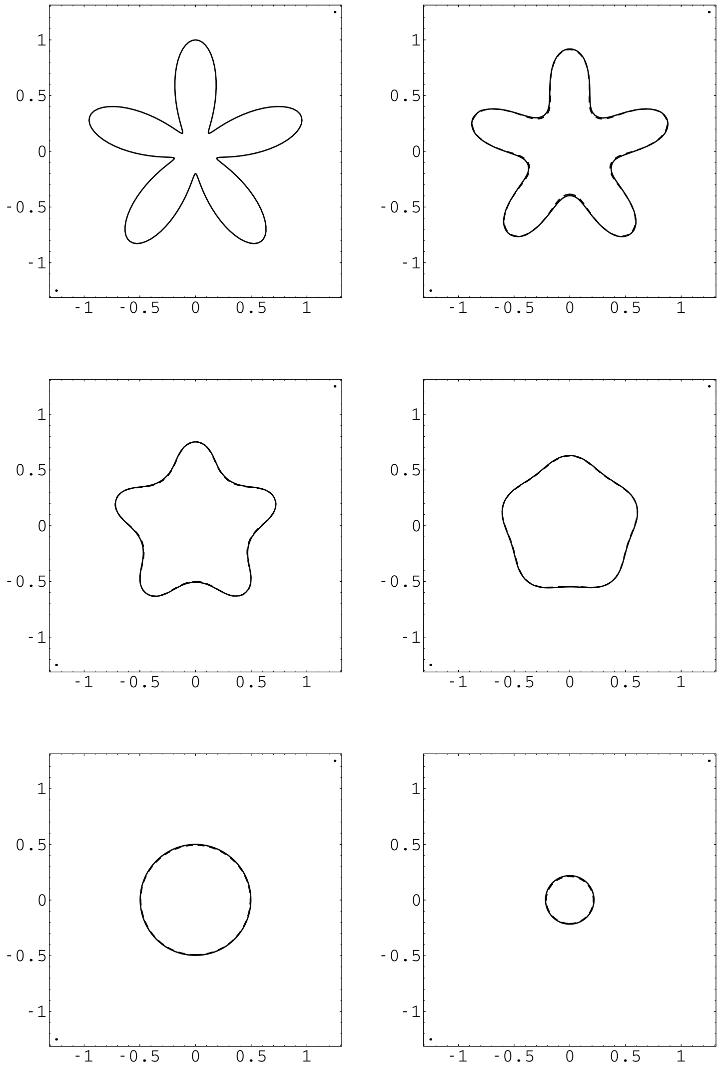

Figure 8. Computational comparison of level set approach and direct approach based on intrinsic heat equation.

5 Phase field approximation of interface motion

As we have mentioned in introduction, the curve evolution equation (1) arises in thermomechanics with interfacial structure, e.g. in the study of phase transitions on microscopic level. If solid occupies a subset $\Omega_s(t) \subset \Omega$ and liquid occupies a subset $\Omega_l(t) \subset \Omega$, $\Omega \subset \mathbb{R}^2$, at a time t, then the phase interface is a set $\Gamma(t) = \partial\Omega_s(t) \cap \partial\Omega_l(t)$ which is assumed to be a closed curve. The sharp-interface description of the solidification process is then described by the Stefan problem with surface tension

$$\rho c \frac{\partial U}{\partial t} = \lambda \Delta U \qquad \text{in } \Omega_s \text{ and } \Omega_l, \tag{26}$$

$$\lambda \frac{\partial U}{\partial N} |_s - \lambda \frac{\partial U}{\partial N} |_l = -Lv \text{ on } \Gamma, \tag{27}$$

$$\frac{\delta e}{\sigma}(U - U^*) = -\alpha_2(\theta)k + \alpha_1(\theta)v \text{ on } \Gamma, \tag{28}$$

accompanied with initial and boundary conditions for temperature field U and initial position of the interface $\Gamma(0)$. The symbols ρ, c, λ represent material characteristics (density, specific heat and thermal conductivity), L is latent heat per unit volume and U^* is a melting point. Discontinuity of heat flux on the interface Γ is described by the Stefan condition (27). The formula (28) is the Gibbs-Thomson relation on Γ, where δe is difference in entropy per unit volume between liquid and solid phases and $\sigma \equiv const$ is surface tension, α_1 is a coefficient of attachment kinetics, and dimensionless function α_2 describes anisotropy of the interface, e.g., it has the form

$$\alpha_2(\theta) = 1 - \zeta \cos(m(\theta - \theta_0))$$

where $\zeta \in [0, 1)$ is a strength of m-fold anisotropy and θ_0 is principal direction - crystallographic orientation.

In [13,14] the following phase-field formulation of (26)–(28) is studied

$$\rho c \tfrac{\partial U}{\partial t} = \lambda \Delta U + L \tfrac{\partial \phi}{\partial t}, \tag{29}$$

$$\alpha_1(\theta)\xi^2 \tfrac{\partial \phi}{\partial t} = \alpha_2(\theta)(\xi^2 \Delta\phi + a\phi(1-\phi)(\phi - 0.5)) + b\tfrac{\delta e}{\sigma}(U^* - U)\xi^2|\nabla\phi| \tag{30}$$

where a, b, ξ are positive model constants. The phase equation (30) is an analogue of the level set formulation

$$\alpha_1(\theta)\frac{\partial \phi}{\partial t} = \alpha_2(\theta)|\nabla\phi|\nabla\left(\frac{\nabla\phi}{|\nabla\phi|}\right) + \frac{\delta e}{\sigma}|\nabla\phi|(U^* - U) \tag{31}$$

of the Gibbs–Thomson condition (28). As it is usual in phase field models the first (degenerate diffusion) term on the right hand side of (31) is

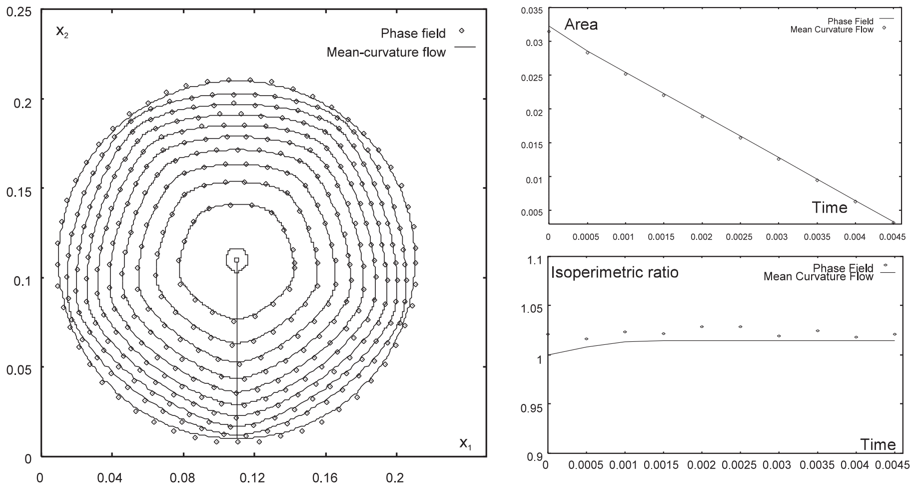

Figure 9. Anisotropic 5-fold mean-curvature flow compared to phase-field model ($\zeta = 0.7$, $F = 0.0$, $a = 4.0$, $\xi = 0.005$, $\alpha_1 = 1$).

replaced by Laplacian and double-well potential term in (30) and moreover the equation depends on small parameter ξ. However, in spite of another phase field formulations, Eq. (30) contains a modified coupling term $b\frac{\delta e}{\sigma}(U^* - U)\xi^2|\nabla\phi| = Fb\xi^2|\nabla\phi|$, which can help in quantitative correspondence of diffusive and sharp interface models. This fact has been observed in intercomparing study of quantitative correspondence of phase field and sharp interface description of mean curvature flow problem [14]. The results of simulations by the phase equation (30) using numerical approximation based on finite difference method has been compared to the results obtained by the method (5)-(7) solving the sharp-interface problem (1). In Figures 9–11 we present comparison which indicates satisfactory correspondence of both models in case of fine enough choice of phase field parameter ξ.

Acknowledgments

The author thanks to M. Beneš, A. Handlovičová, J. Kačur, A. Sarti and D. Ševčovič, whose contribution to development of the presented methods and co-authorship is gratefully acknowledged. The work on this paper was supported by the grant VEGA 1/7132/20 of the Scientific Grant Agency of the Slovak Republic.

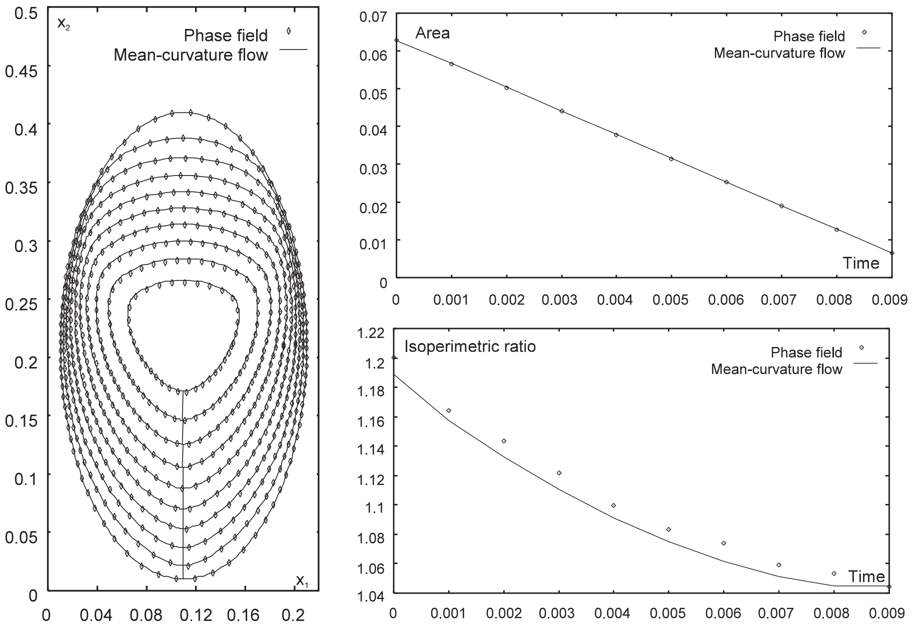

Figure 10. Anisotropic 3-fold mean-curvature flow compared to phase-field model ($\zeta = 0.7$, $F = 0.0$, $a = 4.0$, $\xi = 0.0025$, $\alpha_1 = 1$).

References

1. U. Abresch, J. Langer, The normalized curve shortening flow and homothetic solutions, J. Diff. Geom. **23**, 175 (1986)
2. L. Alvarez, F. Guichard, P.L. Lions, J.M. Morel, Axioms and Fundamental Equations of Image Processing, Arch. Rat. Mech. Anal. **123**, 200 (1993)
3. L. Alvarez, J.M. Morel, Formalization and computational aspects of image analysis, Acta Numerica, 1 (1994)
4. L. Alvarez, P.L. Lions, J.M. Morel, Image selective smoothing and edge detection by nonlinear diffusion II, SIAM J. Numer. Anal. **29**, 845 (1992)
5. B. Andrews, Evolving convex curves, Calculus of Variations and Partial Differential Equations **7**, 315 (1998)
6. S.B. Angenent, On the formation of singularities in the curve shortening flow, J. Diff. Geom. **33**, 601 (1991)
7. S.B. Angenent, Parabolic equations for curves on surfaces I: Curves with

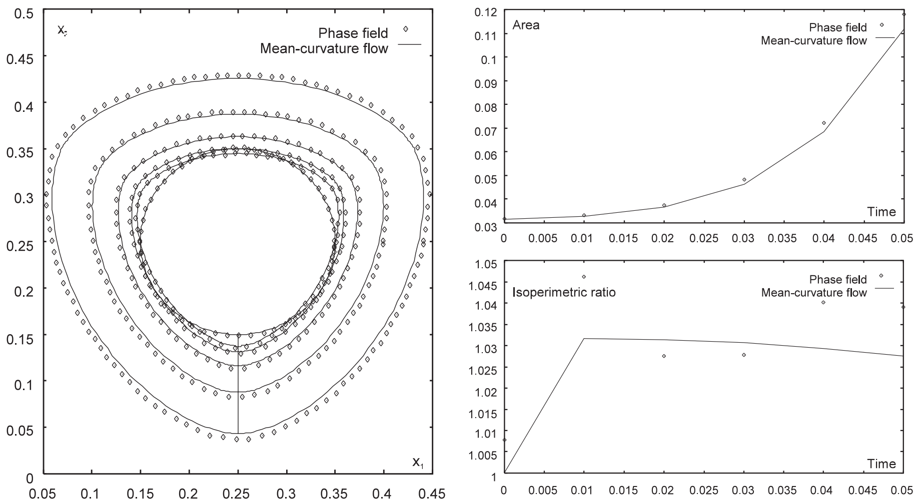

Figure 11. Anisotropic 3-fold mean-curvature flow with force compared to phase-field model ($\zeta = 0.7$, $F = -10.0$, $a = 4.0$, $b = 1$, $\xi = 0.005$, $\alpha_1 = 1$).

p-integrable curvature, Annals of Mathematics **132**, 451 (1990)

8. S.B. Angenent, Parabolic equations for curves on surfaces II: Intersections, blow-up and generalized solutions, Annals of Mathematics **133**, 171 (1991)
9. S.B. Angenent, M.E. Gurtin, Multiphase thermomechanics with an interfacial structure 2. Evolution of an isothermal interface, Arch. Rat. Mech. Anal. **108**, 323 (1989)
10. S.B. Angenent, M.E. Gurtin, Anisotropic motion of a phase interphase. Well-posedness of the initial value problem and qualitative properties of the interphase, J. Reine Angew. Math. **446**, 1 (1994)
11. S.B. Angenent, G. Sapiro, A. Tannenbaum, On affine heat equation for non-convex curves, J. Amer. Math. Soc. **11**, 601 (1998)
12. E. Bänsch, K. Mikula, A coarsening finite element strategy in image selective smoothing, Comput. Visual. Sci. **1**, 53 (1997)
13. M. Beneš, Phase-Field Model of Microstructure Growth in Solidification of Pure Substances, PhD thesis, Faculty of Nuclear Sciences and Physical Engineering, Czech Technical University, Prague, 1997
14. M. Beneš, K. Mikula, Simulations of anisotropic motion by mean curvature – comparison of phase field and sharp interface approaches, Acta Math. Univ. Comenianae **67**, 17 (1998)

15. G. Caginalp, The dynamics of a conserved phase field system: Stefan-like, Hele-Shaw, and Cahn-Hilliard models as asymptotic limits, IMA J. Appl. Math. **44**, 77 (1990)
16. F. Catté, P.L. Lions, J.M. Morel, T. Coll, Image selective smoothing and edge detection by nonlinear diffusion, SIAM J.Numer.Anal. **29**, 182 (1992)
17. Y.-G. Chen, Y. Giga, S. Goto, Uniqueness and existence of viscosity solutions of generalized mean curvature flow equation, J. Diff. Geom. **33**, 749 (1991)
18. V. Caselles, R. Kimmel, G. Sapiro, C. Sbert, Minimal surfaces based object segmentation, IEEE Trans. Pattern Analysis and Machine Intelligence **19**, 394 (1997)
19. M.G. Crandall, H. Ishii, P.L. Lions, User's guide to viscosity solutions of second order partial differential equations, Bull.(NS) Amer. Math. Soc. **27**, 1 (1992)
20. K. Deckelnick, Weak solutions of the curve shortening flow, Calculus of Variations and Partial Differential Equations **5**, 489 (1997)
21. K. Deckelnick, G. Dziuk, Convergence of a finite element method for non-parametric mean curvature flow, Num. Math. **72**, 197 (1995)
22. G. Dziuk, Algorithm for evolutionary surfaces, Num. Math. **58**, 603 (1991)
23. G. Dziuk, Convergence of a semidiscrete scheme for the curve shortening flow, Mathematicals Models and Methods in Applied Sciences **4**, 589 (1994)
24. G. Dziuk, Discrete anisotropic curve shortening flow, SIAM Journal on Numer. Anal. **36**, 1808 (1999)
25. C.M. Elliott, M. Paolini, R. Schätzle, Interface estimates for the fully anisotropic Allen–Cahn equation and anisotropic mean curvature flow, Mathematical Models and Methods in Applied Sciences **6**, 1103 (1996)
26. L.C. Evans, J. Spruck, Motion of level sets by mean curvature I, J. Diff. Geom. **33**, 635 (1991)
27. M. Gage, R.S. Hamilton, The heat equation shrinking convex plane curves, J. Diff. Geom. **23**, 285 (1986)
28. P.M. Girao, Convergence of a crystalline algorithm for the motion of a simple closed convex curve by weighted curvature, SIAM J. Numer. Anal. **32**, 886 (1995)
29. M. Grayson, The heat equation shrinks embedded plane curves to round points, J. Diff. Geom. **26**, 285 (1987)
30. M. Gurtin, Thermomechanics of Evolving Phase Boundaries in the Plane, Clarendon Press, Oxford, 1993

31. A. Handlovičová, K. Mikula, A. Sarti, Numerical solution of parabolic equations related to level set formulation of mean curvature flow, Comput. Visual. Sci. **1**, 179 (1998)
32. W. Jäger, J. Kačur, Solution of porous medium type systems by linear approximation schemes, Num. Math. **60**, 407 (1991)
33. W. Jäger, J. Kačur, Solution of doubly nonlinear and degenerate parabolic problems by relaxation schemes, Mathematical Modelling and Numerical Analysis **29**, 605 (1995)
34. P.L. Lions, Axiomatic derivation of image processing models, Mathematical Models and Methods in Applied Sciences **4**, 467 (1994)
35. J. Kačur, Solution of some free boundary problems by relaxation schemes, SIAM J. Numer. Anal. **36**, 290 (1999)
36. J. Kačur, A. Handlovičová, M. Kačurová, Solution of nonlinear diffusion problems by linear approximation schemes, SIAM J. Numer. Anal. **30**, 1703 (1993)
37. J. Kačur, K. Mikula, Solution of nonlinear diffusion appearing in image smoothing and edge detection, Applied Numerical Mathematics **17**, 47 (1995)
38. J. Kačur, K. Mikula, Slow and fast diffusion effects in image processing, Comput. Visual. Sci. **3**, to appear
39. J. Kačur, K. Mikula, Slowed anisotropic diffusion, in Proceedings of Scale-Space Theory in Computer Vision (ed. by B.t.H.Romeny, L.Florack, J.Koenderink, M.Viergever), Lecture Notes in Computer Science 1252, Springer, 357 (1997)
40. M. Kass, A. Witkin, D. Terzopulos, Snakes: active contour models, International Journal of Computer Vision **1**, 321 (1987)
41. M. Kimura, Accurate numerical scheme for the flow by curvature, Appl. Math. Letters **7**, 69 (1994)
42. M. Kimura, Numerical analysis for moving boundary problems using the boundary tracking method, Japan J. Indust. Appl. Math. **14**, 373 (1997)
43. R. Malladi, J.A. Sethian, B. Vemuri, Shape modeling with front propagation: a level set approach, IEEE Trans. Pattern Analysis and Machine Intelligence **17**, 158 (1995)
44. H. Matano, Non-increase of the lap-number of a solution for a one dimensional semilinear parabolic equation, J. Fac. Sci. Univ. Tokyo Math. **29**, 401 (1982)
45. K. Mikula, Solution of nonlinear curvature driven evolution of plane convex curves, Applied Numerical Mathematics **23**, 347 (1997)
46. K. Mikula, J. Kačur, Evolution of convex plane curves describing anisotropic motions of phase interfaces, SIAM J. Scientific Computing

17, 1302 (1996)
47. K. Mikula, A. Sarti, C. Lamberti, Geometrical diffusion in 3D-echocardiography, in Proceedings of ALGORITMY'97 - Conference on Scientific Computing, West Tatra Mountains - Zuberec, 167 (1997)
48. K. Mikula, Numerical experiments on geometry driven diffusion with application to image processing, in Science and Supercomputing at CINECA, 1997 Report (Ed. M.Voli, CINECA Supercomputing Group), 689 (1998)
49. K. Mikula, N. Ramarosy, Semi-implicit finite volume scheme for solving nonlinear diffusion equations in image processing, Num. Math., to appear
50. K. Mikula, A. Sarti, F. Sgallari, Models and numerical methods for non-linear multiscale analysis of 3D image sequences, submitted
51. K. Mikula, D. Ševčovič, Solution of nonlinearly curvature driven evolution of plane curves, Applied Numerical Mathematics **31**, 191 (1999)
52. K. Mikula, D. Ševčovič, Evolution of plane curves driven by a nonlinear function of curvature and anisotropy, SIAM J. Appl. Math., to appear
53. L. Moissan, Affine plane curve evolution: A fully consistent scheme, IEEE Transactions on Image Processing **7**, 411 (1998)
54. R. Nochetto, M. Paolini, C. Verdi, Sharp error analysis for curvature dependent evolving fronts, Mathematical Models and Methods in Applied Sciences **3**, 711 (1993)
55. K.N. Nordström, Biased anisotropic diffusion - a unified approach to edge detection, Preprint, Department of Electrical Engineering and Computer Science, UC Berkeley (1989)
56. S. Osher, L. Rudin, Feature oriented image enhancement using shock filters, SIAM J. Numer. Anal. **27**, 919 (1990)
57. S. Osher, J.A. Sethian, Front propagating with curvature dependent speed: algorithms based on the Hamilton- Jacobi formulation, J. Comp. Phys. **79**, 12 (1988)
58. M. Paolini, Fattening in two dimensions obtained with a nonsymetric anisotropy: Numerical simulations, Acta Math. Univ. Comenianae **67**, 43 (1998)
59. P. Perona, J. Malik, Scale space and edge detection using anisotropic diffusion, In Proc. IEEE Computer Society Workshop on Computer Vision (Miami Beach, Nov.30-Dec.2,1987), IEEE Computer Society Press, Washington, 16 (1987)
60. Bart M. ter Haar Romeny (Ed.), Geometry driven diffusion in computer vision, Kluwer, Dodrecht, 1994
61. L.I. Rudin, S. Osher, E. Fatemi, Nonlinear total variation based noise removal algorithms, Physica D **60**, 259 (1992)

62. G. Sapiro, A. Tannenbaum, On affine plane curve evolution, J. Funct. Anal. **119**, 79 (1994)
63. G. Sapiro, A. Tannenbaum, Affine invariant scale space, International Journal of Computer Vision **11**, 25 (1993)
64. G. Sapiro, A. Tannenbaum, Invariant curve evolution and image processing, Indiana Univ. Journal of Math. **42**, 985 (1993)
65. G. Sapiro, A. Tannenbaum, Area and length preserving geometric invariant scale-spaces, IEEE Trans. Pattern Analysis and Machine Intelligence **17**, 1066 (1995)
66. A. Sarti, K. Mikula, F. Sgallari, Nonlinear multiscale analysis of 3D echocardiographic sequences, IEEE Transactions on Medical Imaging **18**, 453 (1999)
67. A. Schmidt, Computation of three dimensional dendrites with finite elements, J. Comp. Phys. **125**, 293 (1996)
68. A. Schmidt, Approximation of crystalline dendrite growth in two space dimensions, Acta Math. Univ. Comenianae **67**, 57 (1998)
69. J.A. Sethian, Numerical algotithm for propagating interfaces: Hamilton-Jacobi equations and conservation laws, J. Diff. Geom. **31**, 131 (1990)
70. J.A. Sethian, Level Set Methods. Evolving Interfaces in Geometry, Fluid Mechanics, Computer Vision, and Material Science, Cambridge Monographs on Appl. and Comp. Mathematics, Cambridge University Press, 1996
71. J.A. Sethian, Adaptive fast marching and level set methods for propagating interfaces, Acta Math. Univ. Comenianae **67**, 3 (1998)
72. T. Ushijima, S. Yazaki, Convergence of a crystalline algorithm for the motion of a closed convex curve by a power of curvature $V = K^{\alpha}$, SIAM J. Numer. Anal. **37**, 500 (2000)